

# Pepper (*Capsicum annuum*) xylogen-like arabinogalactan protein (XYLP) 1 and XYLP2 promote synthesis of lignin during stem development to cope with stresses

Min Zhang, Qianwen Zhang, Long Cheng, Qianying Li, Xinyue He, Kaixuan Wang, Jianan Liu, Feng Li, and Yingtian Deng\*

Key Laboratory of Horticultural Plant Biology (Ministry of Education), College of Horticulture and Forestry Sciences, Huazhong Agricultural University, Wuhan 430070, China

\* Corresponding author, E-mail: [dengyt@mail.hzau.edu.cn](mailto:dengyt@mail.hzau.edu.cn)

## Abstract

Pepper stems exhibit a high level of strength and lignin deposition to support plant growth, which direct the cultivation style without binding sticks or scaffolding. However, regulation of lignin synthesis and accumulation in pepper stem has not been extensively studied. Herein, we first investigated the pepper stem developmental process and confirmed that increasing lignin accumulation occurs during stem growth. We then performed genome-wide identification and characterization of xylogen-like arabinogalactan protein (XYLP) family members and obtained 10, 22, and 19 XYLPs in pepper, tomato, and potato respectively. Evaluation of the phylogenetic relationship among the identified XYLPs suggested that these proteins are conserved in *Solanaceae*. Thereafter, we analyzed the 10 CanXYLP genes and observed that these genes exhibit differential expressing patterns at different stages of pepper stem development. Among these genes, two XYLPs, namely CanXYLP1 and CanXYLP2, exhibited an increased expression pattern and a strong correlation with lignin accumulation in pepper stem. We further found that CanXYLP1 and CanXYLP2 play a role in pepper stem lignification by positively regulating the lignin synthesis pathway genes in pepper, and the CanXYLP1/2-silenced plants displayed a blocked lignification phenotype. Finally, we confirmed that CanXYLP1/2 expression is upregulated in response to some abiotic and biotic signals, suggesting that these two genes enhance the tolerance of pepper stem to unfavorable conditions. These results contribute to our understanding of the molecular mechanism controlling pepper stem lignification, and the relationship between the lignin content of pepper stem and XYLPs.

**Citation:** Zhang M, Zhang Q, Cheng L, Li Q, He X, et al. 2022. Pepper (*Capsicum annuum*) xylogen-like arabinogalactan protein (XYLP) 1 and XYLP2 promote synthesis of lignin during stem development to cope with stresses. *Vegetable Research* 2:15 <https://doi.org/10.48130/VR-2022-0015>

## INTRODUCTION

Pepper (*Capsicum annuum*) is a *Solanaceae* plant that is widely cultivated worldwide, which is commonly used as a food source due to its unique flavor and rich nutritional value. Although the seedlings of *Solanaceae* plants such as tomato (*Solanum lycopersicum*), cherry tomato (*Lycopersicon esculentum*), and Chinese lantern (*Physalis alkekengi*) can grow upright at the start, the increase in leaves and emergence of flowers and fruits cause the plants to bend as their stems exhibit low degrees of lignification and mechanical strength. Thus, scaffolds must be set up and branches lifted to promote their growth, which cost substantial human and economic resources. However, most pepper varieties can grow upright during production due to their highly lignified stems. Therefore, the mechanical strength of the pepper stem could be studied to provide guidance for the production of more vegetable crops.

Lignin is one of the main chemical components of plant stem. The accumulation of lignin in the cell wall will affect the mechanical strength of the plant stem<sup>[1]</sup>. As one of the vital secondary metabolites produced by the phenylpropane metabolic pathway, lignin is deposited in the secondary cell wall of all vascular plants. There are several types of monomers which could make up lignin, the three main types being mustard

alcohol, coumarin alcohol, and coniferol, to produce p-hydroxyphenyl (H) lignin, guaiacyl (G) lignin, and syringyl (S) lignin, respectively<sup>[2]</sup>. Lignin mainly contains g-units and a small amount of H-lignin in gymnosperms, whereas G-lignin and S-lignin are the main parts in angiosperms<sup>[3]</sup>. Lignin monomers are produced in the cytoplasm and transported to the ectoplast, before being moved to the cell wall through an ATP-binding cassette transporter to complete polymerization<sup>[4]</sup>. The cell wall rigidity depends on the proportion of these three monophenol units, and the structure of lignin in different plants is not necessarily the same. In recent years, some genes related to lignin biosynthesis have been identified. The total amount of lignin synthesis is closely related to the production and activity level of *phenylalanine ammonia lyase* (PAL)<sup>[5]</sup>, *cinnamate-4-hydroxylase* (C4H)<sup>[6]</sup>, *4-coumarate: CoA ligase* (4CL)<sup>[7]</sup>, *ferulate 5-hydroxylase* (F5H)<sup>[8]</sup>, *caffeic acid/5-hydroxyferulate O-methyltransferase* (COMT)<sup>[9,10]</sup>, *caffeoyl CoA/5-hydroxyferulate CoA-o-methyltransferase* (CCoA-OMT)<sup>[10]</sup>, *cinnamyl alcohol dehydrogenase* (CAD)<sup>[11]</sup>, *p-coumaric acid 3-hydroxylase* (C3H)<sup>[12]</sup>/*hydroxycinnamoyl transferase* (HCT)<sup>[13]</sup>, and *cinnamoyl CoA reductase* (CCR)<sup>[14]</sup>. All the genes listed are crucial for the synthesis of monomers and lignin biosynthesis. The fusion of lignin with cellulose and hemicellulose improves the

mechanical strength and lodging resistance of plant cells. Hu et al.<sup>[15]</sup> reported that lignin content and lignin biosynthetic enzyme activity were crucial in lodging resistance in common buckwheat (*Fagopyrum esculentum*). Studies on cut flowers such as herbaceous peony exhibited that the development of stem increased the degree of lignification, distribution of lignified cell wall, and stem mechanical strength of varieties with a relatively high degree of lignification<sup>[16]</sup>. Additionally, the fusion of substances such as lignin and cellulose in the cell wall skeleton creates an effective barrier to prevent the invasion of various pests and pathogens, and improve the cellular defense ability of plants<sup>[17]</sup>.

Arabinogalactan proteins (AGPs) are a high molecular weight glycoprotein commonly existing in the plant kingdom, which are composed of a protein core skeleton and glycosyl side chain<sup>[18,19]</sup>. AGP responds to abiotic stress factors<sup>[20]</sup> and participates in the regulation of various hormones such as cytokinin<sup>[21]</sup>, abscisic acid<sup>[22]</sup>, and gibberellin<sup>[23]</sup>. The protein skeleton mainly contains substantial hydroxyproline/proline, alanine, serine, and threonine, while the different additional domain could divided AGPs into classical AGPs, lysine rich AGPs, Ag peptides, hybrid AGPs, and chimeric AGPs<sup>[24]</sup>. Among them, Xylogen-like arabinogalactan protein (XYLP) is a kind of chimeric AGP, comprising an additional lipid transfer protein (nsLTP) domain<sup>[25]</sup>. Previous studies exhibited the crucial role of XYLPs during the development of vascular system in *Arabidopsis*<sup>[25]</sup>, rice (*Oryza sativa* L.)<sup>[26]</sup>, wine grape (*Vitis vinifera* L.)<sup>[27]</sup>, poplar (*Pinus taeda* L.)<sup>[28]</sup> and zinnia (*Zinnia elegans* L.)<sup>[29]</sup>. Especially the notable function of XYP1 and XYP2 in *Arabidopsis*, with the *xyp1xyp2* double mutant displaying discontinuous veins in roots, cotyledons and leaves caused by the obvious morphological defects in vascular development<sup>[25]</sup>. *Osxylp7* mutants exhibit shorter stems and panicle stem lengths in rice, and *OxXYLP7* could be up-regulated not only under abiotic stresses such as drought and salt stress, but also under NAA, IAA and 6-BA treatments<sup>[26]</sup>. In grape, *VvXYLP02* was found to be induced by JA upon the pathogen infection, and participate in plant resistance against gray mold disease<sup>[30]</sup>. *PtXYLP1* and *PtXYLP2* are transcriptionally regulated by NAA, 6-BA and GA during *Arabidopsis* cotyledon development<sup>[28]</sup>. These results indicate that XYLPs could play important roles in plant growth and under stress. Therefore, analysis of XYLP could provide theoretical significance for understanding the mechanism of plant vascular system.

## MATERIALS AND METHODS

### Plant material observation and treatment

Pepper cultivars 'ST-8' and 'HP' were used in this study, with all of the pepper plants being cultivated at 80–100  $\mu\text{mol photons m}^{-2}\text{s}^{-1}$ , a relative humidity of 70%, and under a 16/8 h day/night photoperiod in the greenhouse. The pepper cultivar 'ST-8' were grown in the greenhouse at 25 °C. 'ST-8' plants were observed from 2 weeks after germination (W) every two weeks until 12 weeks. Stems at each stage at the position between the pair of cotyledons and first true leaves were sampled for observation or left in liquid nitrogen and stored at  $-80\text{ }^{\circ}\text{C}$  until use. Three independent biological replicates were performed each time. The pepper cultivar 'HP' was used in VIGS (virus-induced gene silencing) to observe the phenotype of *TRV2:CanXYLP1* and *TRV2:CanXYLP2*<sup>[31]</sup>. 'HP' was grown in the

greenhouse at 25 °C before 2 weeks after germination, and then transferred to  $17 \pm 1\text{ }^{\circ}\text{C}$  after 2 weeks for VIGS. Regarding the stress treatment, 2 weeks after VIGS treatment, when the parallel *TRV2:PDS* control started bleaching, plants were put under 10 °C for cold stress, or left with watering reduced by half for drought stress for 1 month. The photographs of whole plants were taken using a digital camera (Nikon, D7500), and the stem images were taken under the microscope (Leica, M205FA).

### Lignin staining and extraction

To stain the lignified area in the stem cross section, we placed cut pepper stems on glass slides, and added 50–100  $\mu\text{l}$  of hydrochloric acid (Baiaolaibo, Beijing, GL2679). After the stem was saturated, we added the same amount of phloroglucinol (Baiaolaibo, Beijing, China GL2679). The lignified cell wall was then stained. After taking the images under a microscope (Leica, M205FA), we used Image J software (<https://imagej.nih.gov/ij/>) to quantify the stained area. The data are presented as the means  $\pm$  SD; 20–30 independent biological replicates.

To extract and test the lignin content, we followed the method established by Cuzens & Miller<sup>[32]</sup>. Firstly, we took an appropriate amount of pepper stems, dried them at 40 °C overnight and ground them into a powder. We then extracted ground powders using a benzene-ethanol solution and hydrolyzed them with 67.0%  $\text{H}_2\text{SO}_4$ . Klason lignin was separated as insoluble matter. We then placed the residues after filtration and ashed them in the Muffle furnace (Daoux, Zhejiang, China SX2-2.5-10) at  $575 \pm 25\text{ }^{\circ}\text{C}$  for 4 h. Finally, we calculated the Klason lignin content by comparing the weight before and after. The data are presented as the means  $\pm$  SD; of three independent biological replicates.

### Identification of XYLPs and bioinformatics analysis

Following the method established by Ma & Zhao<sup>[33]</sup>, *CanXYLP*, *SlyXYLP* and *StuXYLP* proteins were identified respectively (see Supplemental Method for details). An unrooted phylogenetic tree was constructed using MEGA7<sup>[34]</sup> with the neighbor-joining statistical method and bootstrap analysis (1,000 replicates). The software MCScan X<sup>[35]</sup> was used to identify the XYLP orthologous genes between pepper and tomato. The possible regulatory elements of the *CanXYLP1* and 2 gene promoter sequence were analyzed through the promoter regulatory element prediction website PlantCARE (<https://bioinformatics.psb.ugent.be/webtools/plantcare/html/>)<sup>[36]</sup>.

### Pepper VIGS

The pepper VIGS approach was carried out as per the method of Zhou et al.<sup>[31]</sup>. The fragments of *CanXYLP1* and *CanXYLP2* with a length of about 250 bp were inserted into the *TRV2-C2b* vector at the *SmaI* site to construct two vectors, *TRV2:CanXYLP1* and *TRV2:CanXYLP2*, as well as the *CanPDS* gene was inserted into *TRV2* empty vector to construct a positive control *TRV2:CanPDS*. *TRV1* and *TRV2:CanXYLP1/TRV2:CanXYLP2/TRV2:CanXYLP1 + TRV2:CanXYLP2/TRV2:CanPDS* (resuspended in induction medium at a 1:1 ratio,  $\text{OD}_{600} = 0.004$ ), were co-infiltrated into the cotyledon of 'HP' pepper at 2 weeks, and then cultivated at  $17 \pm 1\text{ }^{\circ}\text{C}$  under 16/8 h day/night photoperiod. At 10 weeks, phenotypic observation and sampling of plants were carried out for RNA isolation, RNA-seq and quantitative real-time PCR. Three independent biological replicates

## CanXYLP1 and 2 function on stem lignification

for RNA isolation and quantitative real-time PCR were taken, two of which were used for RNA-seq.

### RNA isolation, cDNA synthesis and quantitative real-time PCR

Total RNA was isolated using TransZol (TransGen Biotech, Beijing, China). Approximately 1  $\mu$ g of total RNA was used for cDNA synthesis through reverse transcription enzyme (Applied Biological Materials Inc., Richmond, Canada). The relative gene expression was calculated using the  $2^{-\Delta\Delta CT}$  method. A pepper Beta-tubulin gene (CA04g21850) was used as the internal controls. The primers used for qRT-PCR are listed in [Supplemental Table S1](#). In each case, three technical replications were performed for each of the three independent biological replicates.

### RNA-seq data analysis

Comparing RNA-seq reads with Hisat2 (<http://daehwankim-lab.github.io/hisat2/>) to convert the sam file, and then using Samtools (<http://samtools.sourceforge.net/>) to bam and sort it, next using FeatureCounts (<http://subread.sourceforge.net/>) to get the count value and finally calculate the FPKM (Fragments per Kilobase Million) value. Differentially expressed gene analysis was conducted using the R package limma (<https://bioconductor.org/packages/release/bioc/html/limma.html>) and edgeR (<https://bioconductor.org/packages/release/bioc/html/edgeR.html>). Genes that exhibited a difference of at least twofold with a corrected P value  $\leq 0.05$  were regarded as significantly differentially expressed. Online enrichment analysis of differential genes used KEGG ([www.kegg.jp](http://www.kegg.jp)). Venn diagrams were drawn by DeepVenn ([www.deepvenn.com](http://www.deepvenn.com)) online. Volcano plots and heat maps were drawn by Tbttools<sup>[37]</sup>.

### Data analysis and software

All the statistical analyses in this study were performed using IBM SPSS Statistics for Windows, version 23.0 (IBM Corp., Armonk, NY, USA). Variance and significant difference tests were carried out to identify differences among means by one-way analysis of variance (ANOVA) with Duncan's multiple range test. The histograms were generated via GraphPad Prism 8.0.2 (GraphPad Software, San Diego, CA, USA), Excel 2019 (Microsoft, Redmond, WA, USA) and OriginPro 2021 (OriginLab, Northampton, MA, USA) software to draw charts.

## RESULTS

### Lignin content gradually increase during pepper stem growth

The present study systemically investigates pepper ST-8's stems at different growth stages from 2 weeks after germination (W) to 12 weeks to determine the lignin content during pepper stem development ([Fig. 1a](#)). The transverse growth of the stem is obvious during pepper plant development ([Fig. 1ai & ii](#)), whereas the xylem area and lignin content increases gradually ([Fig. 1aiii & iv, arrows](#)) ([Fig. 1b](#)). The lignin content in pepper stems was rarely detected at 2 weeks, whereas it reached the peak at 10 weeks. The present study observed the lignin area in stem by specific staining using phloroglucinol hydrochloric acid reagent to further study the soft stem at 4 weeks and hard stem at 10 weeks. The cross-section of the 4 week pepper stem exhibited four regular and small red spots ([Fig. 1c](#)), whereas the cross-section of the 10 week pepper stem exhibited a dark red and circle area filled with lignin ([Fig. 1d](#)).

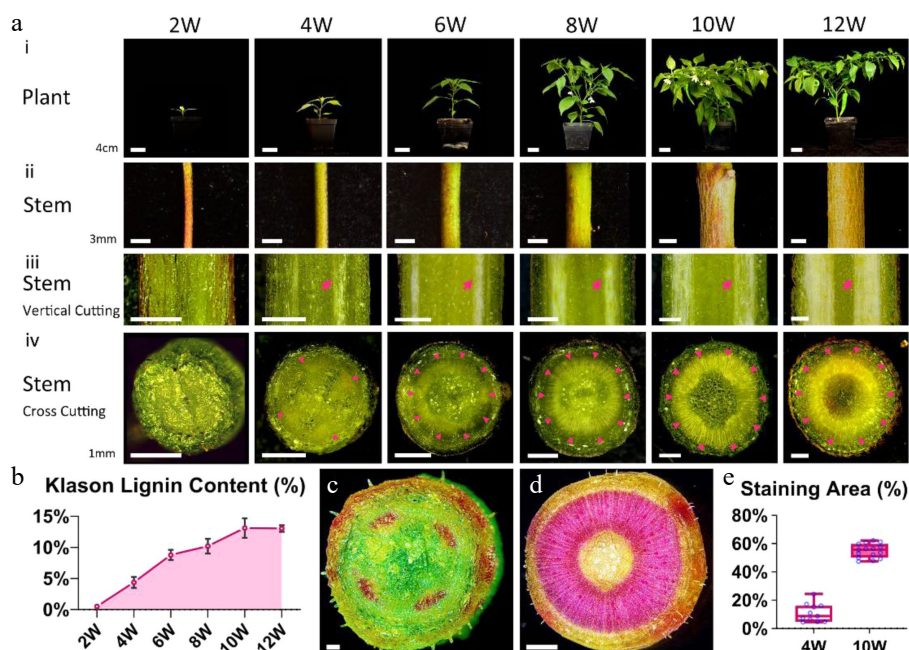


**Fig. 1** The contents of lignin increase during pepper stem development. (a) Pepper plant and stem from 2 weeks after germination 2W to 12W: (i) the whole plant morphology of pepper. Bars = 4 cm. (ii) Magnified images of pepper stems. Bars = 3 mm. (iii) Vertical Cutting of pepper stems under stereomicroscope. Red arrows indicate the position of the xylem. Bars = 1 mm. (iv) Cross Cutting of pepper stems under stereomicroscope. Red arrowheads indicate the position of the xylem. Bars = 1 mm. (b) Klason lignin contents in pepper stems from 2W to 12W. (c), (d) Cross section of pepper stem stained with phloroglucinol hydrochloric acid staining solution at 4W (c, bar = 0.2 mm) and 10W (d, bar = 1 mm) under stereomicroscope. (e) The ratio of the area stained by the phloroglucinol hydrochloric acid staining solution to the entire cross-section at 4W and 10W.

These staining areas were also quantified and exhibited a significant difference (Fig. 1e). Therefore, we concluded that the lignin content in the pepper stem increased gradually during growth to provide the pepper stem the essential mechanical strength.

**Identification and characterization of XYLP family members in pepper**

BLASTP searches were performed across pepper protein databases (zunla2.0)<sup>[38]</sup> using ZeXYP1, AtXYP1, and AtXYP2 protein sequences as queries to identify XYLPs in pepper<sup>[25]</sup>. After confirming the presence of nsLTP-like domains, AGP-like regions, and AG-type glycomodules, and removing redundant sequences, 10 CanXYLPs were identified in pepper (Supplemental Table S2 and S3). Compared with ZeXYP, AtXYP1, and AtXYP2 protein sequences, all 10 CanXYLPs were predicted to possess an N-terminal signal peptide for targeting the

endoplasmic reticulum and a C-terminal GPI anchor protein (Fig. 2a and Supplemental Table S2). Additionally, putative AG glycomodules in all CanXYLPs were distributed in the PAST-rich region before and after the nsLTP-like domain. N-glycosylation sites in most of the CanXYLPs were located in the nsLTP-like domain and the PAST-rich region (Fig. 2a and Supplemental Table S3). The existence of signal peptides and AG glycomodules suggested that the 10 CanXYLPs may be chimeric AGPs. To further study the XYLP protein specific feature, the nsLTP-like domains of the above XYLPs were aligned. The distribution of eight cysteine (C) residues was highly conserved with the formation of a C-X-C-X-CC-X-CX-C-X-C-X-C region, whereas the hydrophobicity of the residue between 5<sup>th</sup> C and 6<sup>th</sup> C was also conserved with leucine (L), except CanXYLP2 and tyrosine (Y) (Fig. 2a and Supplemental Fig. S1). The conserved nsLTP-like domain was involved in the formation of a three-dimensional

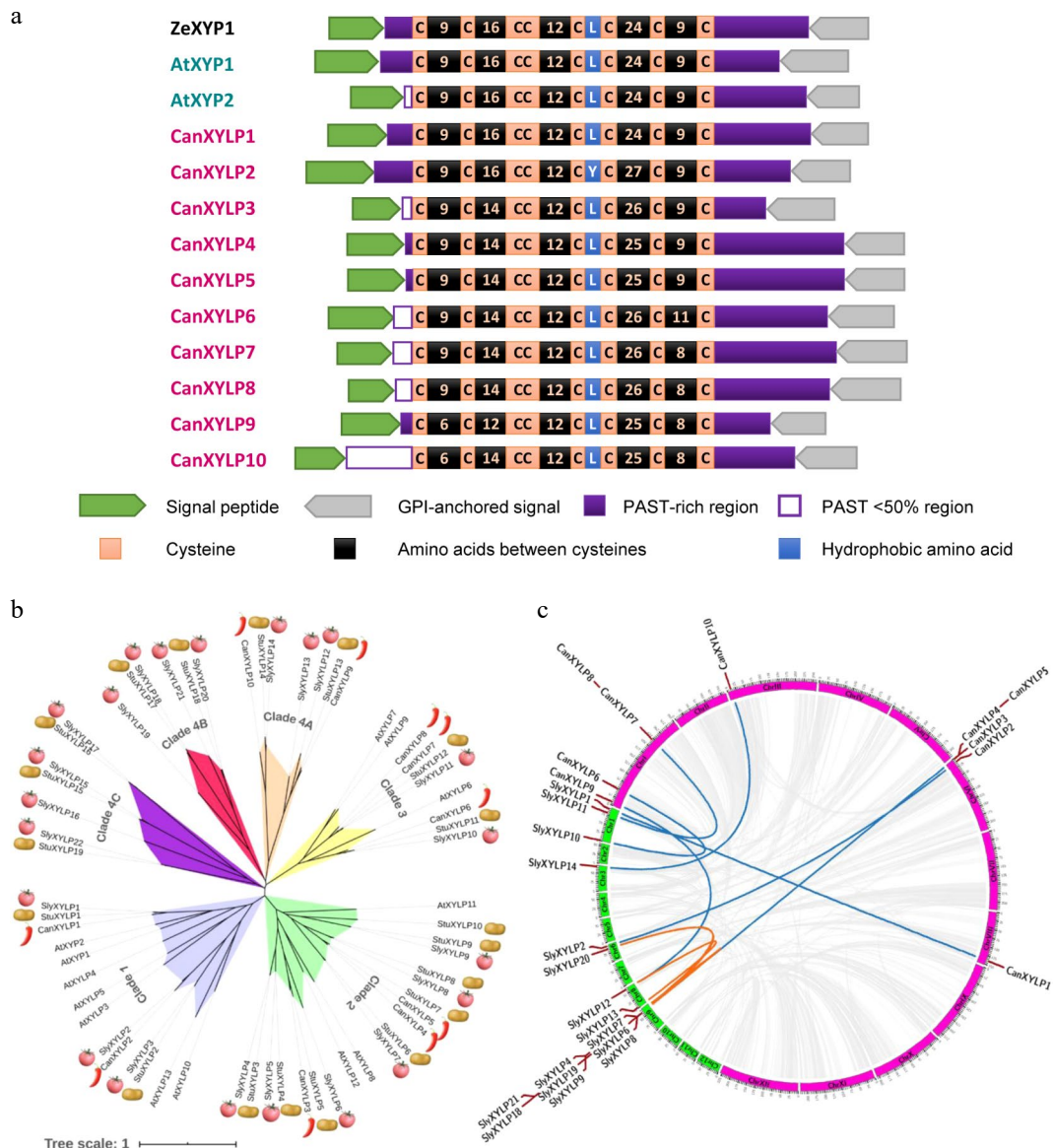


**Fig. 2** Protein structure, Phylogenetic and synteny relationship of XYLPs in Solanaceae. (a) Conserved motifs and structure domain of ZeXYP1, AtXYP1, 2 and 10 CanXYLP proteins. (b) Phylogenetic tree of 12 AtXYLPs, 22 SlyXYLPs, 19 StuXYLPs and 10 CanXYLPs. (c) Comparative synteny of the XYLP gene family between pepper and tomato. Blue lines show interspecific collinearity relationship, orange lines show intraspecific collinearity relationship and gray lines show collinearity relationship of all genes.

## CanXYLP1 and 2 function on stem lignification

structure that could firmly bind lipids, implying their crucial ability to bind or transfer various types of hydrophobic molecules such as fatty acids, fatty acyl-CoA, phospholipids, glycolipids, and cutin monomers *in vitro*<sup>[38]</sup>.

Phylogenetic and synteny analysis of XYLPs in *Solanaceae*

The present study identified 22 SlyXYLP proteins in tomato (*Solanum lycopersicum*) and 19 StuXYLP proteins in potato (*Solanum tuberosum*) to fully understand the XYLPs among nightshade (Supplemental Table S2). The *Solanaceae* XYLP protein full sequences were then used with 13 well-known AtXYLPs to obtain an unrooted phylogenetic tree exhibiting their phylogenetic relationships (Fig. 2b). According to the sequence homology of proteins, CanXYLPs, SlyXYLPs, StuXYLPs, and AtXYLPs proteins were divided into four independent evolutionary clades (1–4), and the family members with high sequence homology were divided into the same clade. Clades 1, 2, and 3 contained XYLPs from these four species, whereas clade 4 is nightshade specific, comprising three sub-clades (A–C). Clade 4B and 4C mainly contain XYLP protein from tomato and potato. The phylogenetic tree exhibited that the XYLP protein underwent different evolutionary pathways after the differentiation of *Arabidopsis* and *Solanaceae* plants. Additionally, the XYLP protein in Clade 4 can only appear in *Solanaceae* plants, indicating that the XYLP proteins of these subfamilies were isolated later.

Large-scale comparative synteny maps were analyzed at genome-wide levels to reveal the mechanism for expansion and evolution of the XYLP gene family between pepper and tomato (Fig. 2c). Eight pairs of XYLP genes were identified between pepper and tomato (Fig. 2c, blue lines and Supplemental Table S4) exhibited interspecific collinearity relationships, suggesting that most CanXYLPs were orthologous in tomato. Additionally, among the synteny events, six intraspecific collinearity pairs of XYLP genes were observed in tomato (Fig. 2c; orange lines and Supplemental Table S4), which were not observed in pepper, indicating more XYLP duplication in tomato.

Expression patterns of *CanXYLP* genes during pepper stem development

The real-time quantitative reverse-transcription polymerase chain reaction (qRT-PCR) was conducted to measure their relative expression levels at different stages of stem development to elucidate the roles of CanXYLPs in stem development (Fig. 3). The stems of six stages were harvested from 2 weeks to 12 weeks after germination. The expression levels of 10 *CanXYLP* genes during stem development could be divided into three categories, namely the expression levels of *CanXYLP1*, 2, and 10, which were gradually increased during stem development and reached the peak at 12 weeks. On the other hand, *CanXYLP7* and 8 were highly expressed in the early stage and then gradually decreased with plant growth, suggesting that these genes may be closely related to stem lignification. Both *CanXYLP3* and 9 exhibited an expression peak at 4 weeks, whereas *CanXYLP4*, 5, and 6 groups peaked at 6 weeks. The two pair of tandem replication genes, *CanXYLP4* and 5, and *CanXYLP7* and 8, exhibited the same expression pattern, indicating that they may have the same biological function. The different expression pattern of these 10 *CanXYLP* genes during pepper stem growth indicated their different function in this process.

Virus induced gene silencing of *CanXYLP1/2* leading to reduced lignin contents in pepper stem

Previous studies have exhibited the vital role of AtXYP1 and AtXYP2 in vascular development<sup>[25]</sup>. The present study focused on CanXYLP1 and CanXYLP2 to explore their function in pepper. By using the virus-induced gene silencing (VIGS) approach, we have either *CanXYLP1* (*TRV2:CanXYLP1*) or *CanXYLP2* (*TRV2:CanXYLP2*), as well as both of *CanXYLP1* and 2 gene silenced pepper 'HP' plants (*TRV2:CanXYLP1+2*) (Fig. 4a). The qRT-PCR results exhibited that the *CanXYLP1* and *CanXYLP2* gene expression decreased in these VIGS plants (Fig. 4d, e). As a technical marker, the PDS (Phytoene desaturases) gene-silenced plant exhibited bleaching of the leaves and stem (Fig. 4b, c), indicating that the VIGS method was effective and could be used for stem development analysis. All of the stems from *TRV2:CanXYLP1*, *TRV2:CanXYLP2*, and *TRV2:CanXYLP1+2* plants

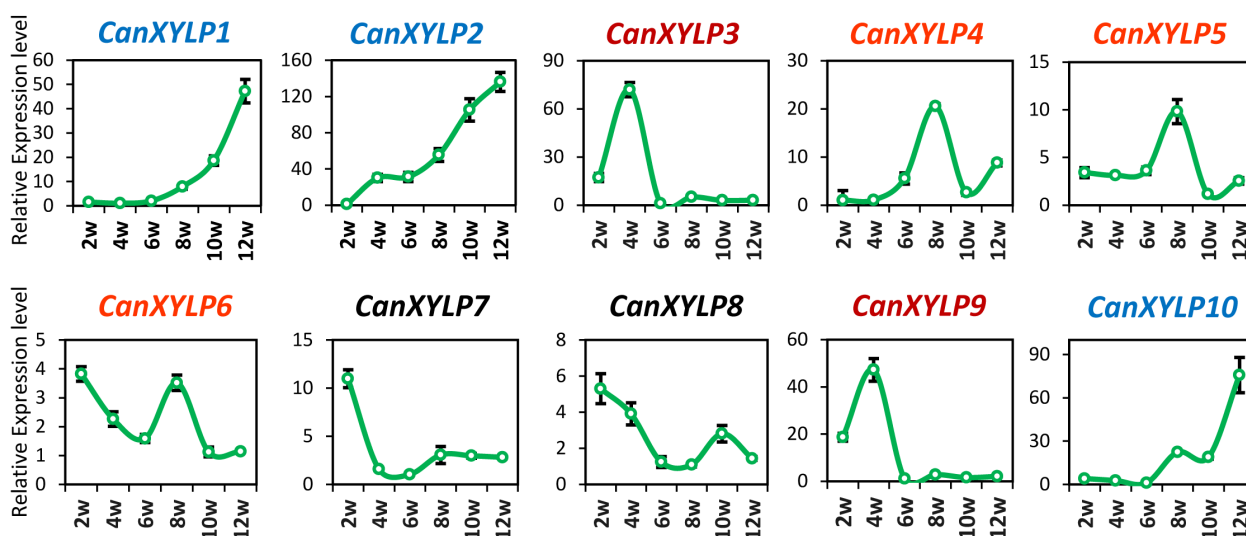


**Fig. 3** Expression analysis of *CanXYLP* genes during pepper stem growth. Relative expression level of 10 *CanXYLP*s in the stems of pepper at 6 developmental stages from 2W to 12W.

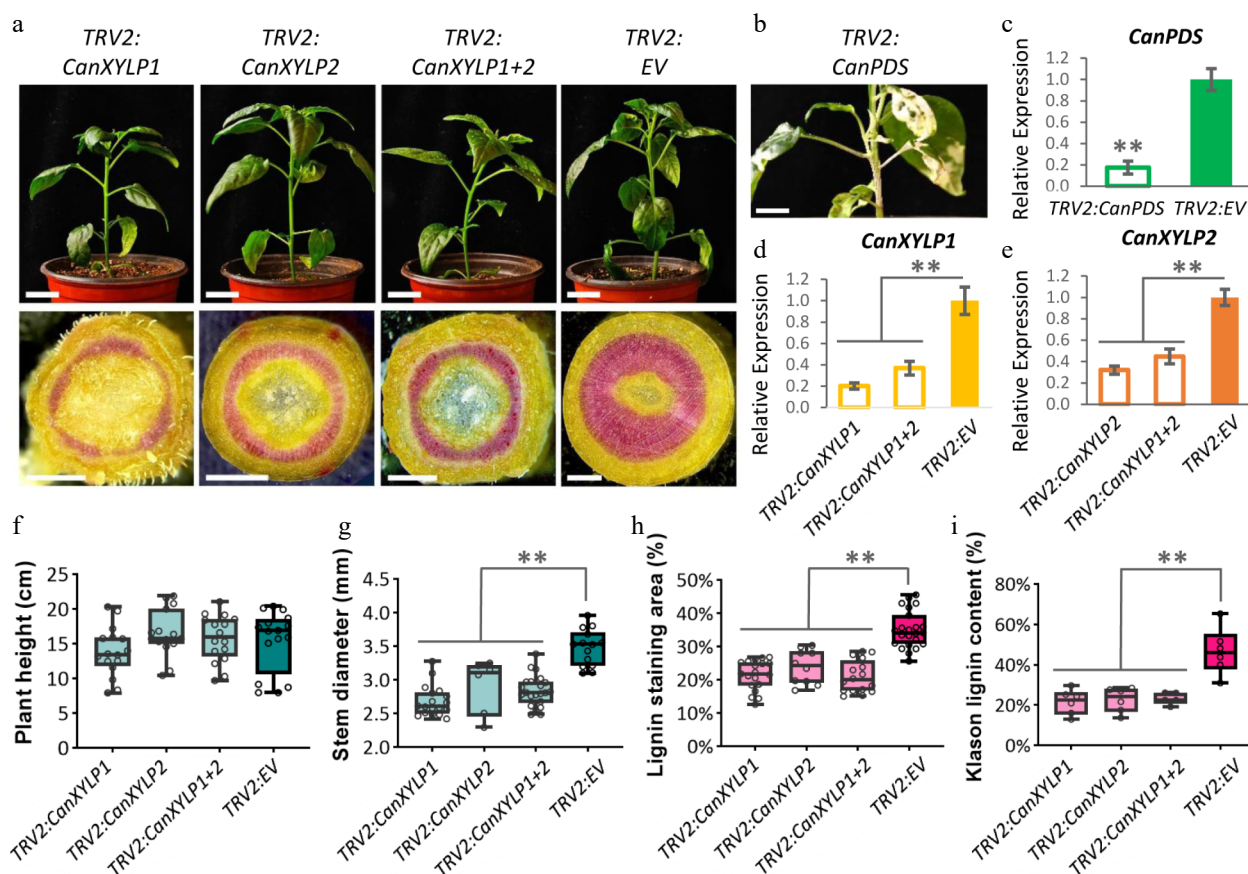


**Fig. 4** *CanXYLP1* and 2 silencing significantly reduced the lignin contents in pepper stem. (a) Phenotypes of *TRV2:CanXYLP1/TRV2:CanXYLP2/TRV2:CanXYLP1+2/TRV2:EV + TRV1* expressed pepper plants (Bars = 2 cm) and the cross sections of their stems (Bars = 1 mm) at 10W stage. (b) Bleached stem of pepper plant expressed *TRV2:CaPDS*. Bar = 2 cm. (c) Relative expression of *CanPDS* gene after *TRV2:CanPDS/TRV2:EV + TRV1* infiltrated stems at 10W stage. (d) Relative expression of *CanXYLP1* in *TRV2:CanXYLP1/TRV2:CanXYLP1+2/TRV2:EV + TRV1* infiltrated stems at 10W stage. (e) The relative expression of *CanXYLP2* in *TRV2:CanXYLP2/TRV2:CanXYLP1+2/TRV2:EV + TRV1* infiltrated stems. (f)–(i) Comparison of plant height (f), stem diameter (g), ratio of area stained by phloroglucinol hydrochloric acid to the entire cross section (h) and Klason lignin content (i) among *TRV2:CanXYLP1+TRV1*, *TRV2:CanXYLP2 + TRV1*, *TRV2:CanXYLP1+2 + TRV1* and *TRV2:EV + TRV1* infiltrated stems at 10W stage (\*\*, P < 0.01).

were much thinner than the negative control *TRV2:EV* (Fig. 4a, g), which might be due to the blocked xylem development. Thus, we next investigated the lignin content in these stems, and a significant decrease was observed in the *CanXYLP1/2*-silenced plants (Fig. 4a, h). Furthermore, the region with less lignin was demonstrated after phloroglucinol hydrochloric acid staining (Fig. 4a, i), indicating that both *CanXYLP1* and 2 are necessary during pepper stem development and lignification, and the loss of either of them will affect lignin biosynthesis.

#### Downregulation of lignin biosynthesis genes in *CanXYLP1/2*-silenced plants

The knockdown of either or both *CanXYLP1* and *CanXYLP2* exhibited an obviously narrowed stem phenotype and inhibition of lignin production. The expression of some genes associated with lignin biosynthesis might be changed. Therefore, RNA Sequencing (RNA-seq) was conducted to discover the differentially expressed genes (DEGs) from the stem samples of *TRV2:CanXYLP1* (TX1), *TRV2:CanXYLP2* (TX2), *TRV2:CanXYLP1+2* (TX1\_2), and *TRV2:EV* (EV) at 10W. The RNA-seq experiment was repeated with two independent biological replications. The RNA-seq approach produced approximately 10 Gb of data for each sample and approximately 93% of the reads were mapped

to the pepper genome (Supplemental Table S5 and Supplemental Fig. S2a), ensuring that the RNA-seq results were relatively credible. Thousands of genes were specifically differently expressed in TX1, TX2, and TX1\_2 compared with the EV. There were 3,113 upregulated DEGs and 3,311 downregulated DEGs in the TX1 compared with the EV, 2,839 upregulated DEGs and 2,138 downregulated DEGs in the TX1 compared with the EV, and 1,910 upregulated DEGs and 1,394 downregulated DEGs in the TX1\_2 compared with the EV (Fig. 5b). Overlapping data were chosen for further analysis due to data redundancy among TX1/EV, TX2/EV, and TX1\_2/EV. Finally, 651 upregulated DEGs and 914 downregulated DEGs were obtained by sequencing (Fig. 5c). Then, the DEG data were used to identify the weakened gene expression profiles involved in the phenylpropanoid metabolic pathway in the TX1, TX2, and TX1\_2 samples to explore the relationship between DEGs and lignin biosynthesis by KEGG (Kyoto Encyclopedia of Genes and Genomes) analysis (Supplemental Fig. S2b). Additionally, the transcript levels of the genes sharply decreased in all of TX1, TX2, and TX1\_2 samples, including most essential enzymes that make up the lignin biosynthesis pathway (Fig. 5a and Supplemental Table S6). Furthermore, the qRT-PCR results for

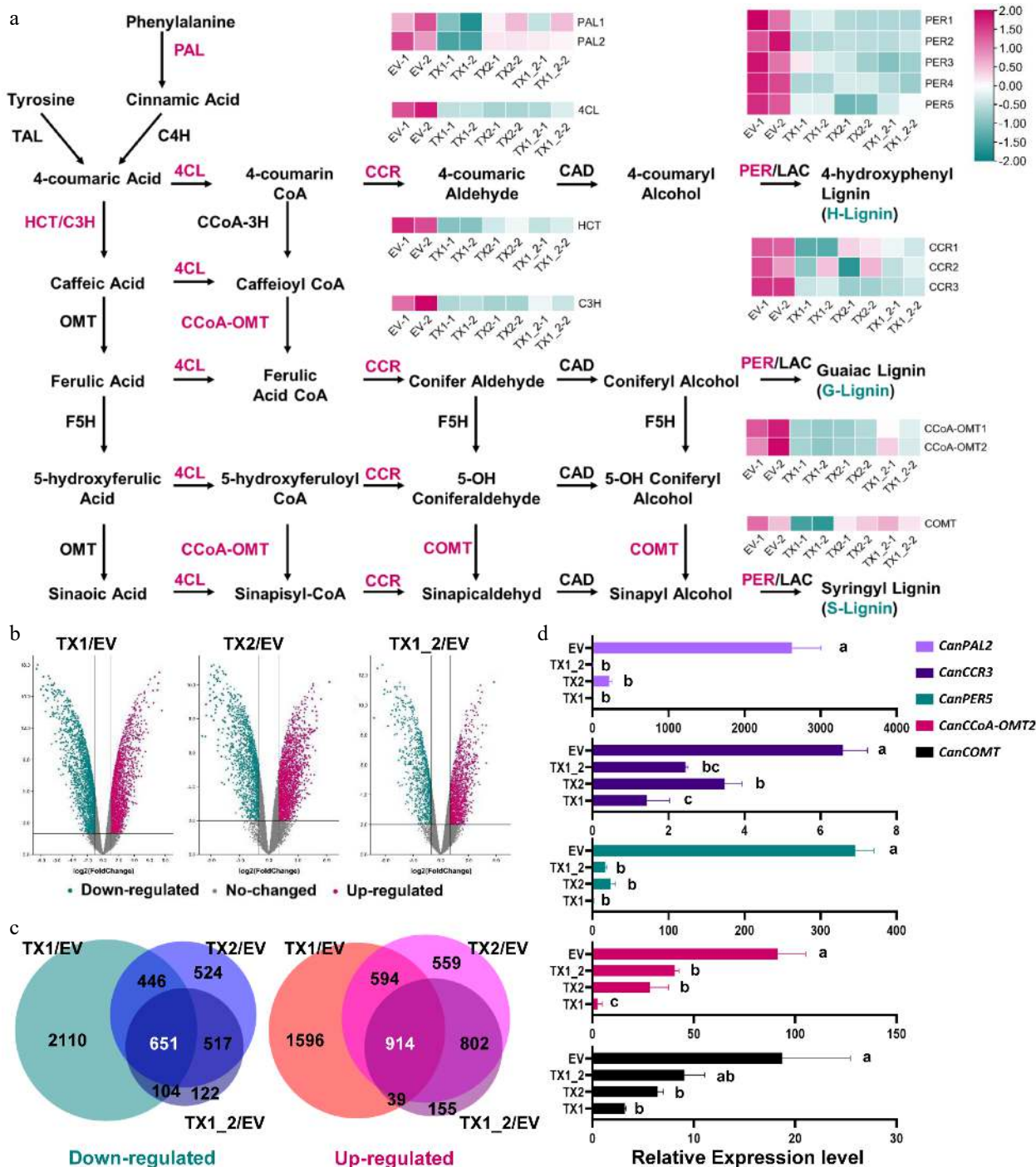


**Fig. 5** CanXYLP1 and 2 function on lignin synthesis pathway in pepper. (a) Heatmap of transcript levels in FPKM for genes that are involved in the lignin biosynthetic pathway and are distinctly expressed among TX1, TX2, TX1\_2 and EV. (b) Volcano plot of DEGs. Red dots indicate up-regulation, blue dots indicate down-regulation, gray dots indicate unchanged. (c) Venn diagram analysis of lower (left) and higher (right) expressed genes in TX1/EV, TX2/EV and TX1\_2/EV. (d) qRT-PCR analysis verified the down-regulated relative expression levels of CanPAL2, CanCCR3, CanPER5, CanCCoA-OMT2 and CanCOMT in TX1, TX2, TX1\_2 compared with EV ( $P < 0.05$ ).

*CanPAL2*, *CanCCR3*, *CanPER5*, *CanCCoA-OMT2*, and *CanCOMT* were consistent with the FPKM (Fragments per Kilobase Million) results (Fig. 5d), indicating that the gene downregulation related to lignin biosynthesis was consistent with the lignin content being dramatically reduced due to loss of function of CanXYLP1/2.

### CanXYLP1 and 2 gene response to biotic and abiotic stresses

The cis-regulatory elements in *CanXYLP1* and *CanXYLP2* promoter sequences were analyzed to further study the upstream regulation mechanism of *CanXYLP1* and *CanXYLP2* genes. The promoter regions (1,500 bp of genomic DNA sequence)

upstream of the translation starts site were submitted in the PlantCARE database<sup>[36]</sup>. In addition to the basic TATA and CAAT boxes, a large number of cis-acting elements involved in biotic and abiotic stresses were identified both in the promoter of CanXYLP1 and CanXYLP2 (Fig. 6a), including cold (Fig. 6a, green triangles), drought (Fig. 6a, dark blue triangles), ABA (Fig. 6a, red triangles), GA (Fig. 6a, orange triangles), and JA (Fig. 6a, light blue triangles), suggesting that these two genes may respond to the stresses. Then, the expression pattern of CanXYLP1 and CanXYLP2 in roots was investigated after biotic and abiotic treatment in the Pepperhub database<sup>[39]</sup>. Thus, the expression level of both CanXYLP1 and CanXYLP2 was activated after treated for 1–6 h (Fig. 6b, c). Additionally, qRT-PCR assay proved that compared with the mock treatment, CanXYLP1 and CanXYLP2 genes exhibited an increased expression under all the five treatments (Fig. 6d, e). Thus, CanXYLP1 and CanXYLP2 genes could be upregulated by biotic and abiotic signals, indicating that lignin could protect plants from various stresses.

Additionally, the MYB transcriptional factor binding element was also observed in the promoter region of both CanXYLP1 and CanXYLP2 genes (Fig. 6a, purple triangles), suggesting that CanXYLP1 and CanXYLP2 participate in the lignin biosynthesis in pepper stem through MYB regulation.

## DISCUSSION

Xylogen is a glycoprotein involved in the differentiation of tracheary element (TE) and local intercellular communication. XYLPs are xylogen-like AGPs characterized by an AGP domain and a plant nsLTPs domain<sup>[29]</sup>. The present study identified 10, 22, and 19 XYLPs in pepper, tomato, and potato, respectively (Fig. 2b). All of the XYLP protein structures were well-characterized with specific AGP and nsLTPs domain (Supplemental Fig. S1, Supplemental Table S2), indicating that the XYLPs were conserved in Solanaceae. To investigate the relationship of XYLPs and enhanced lignification during pepper stem

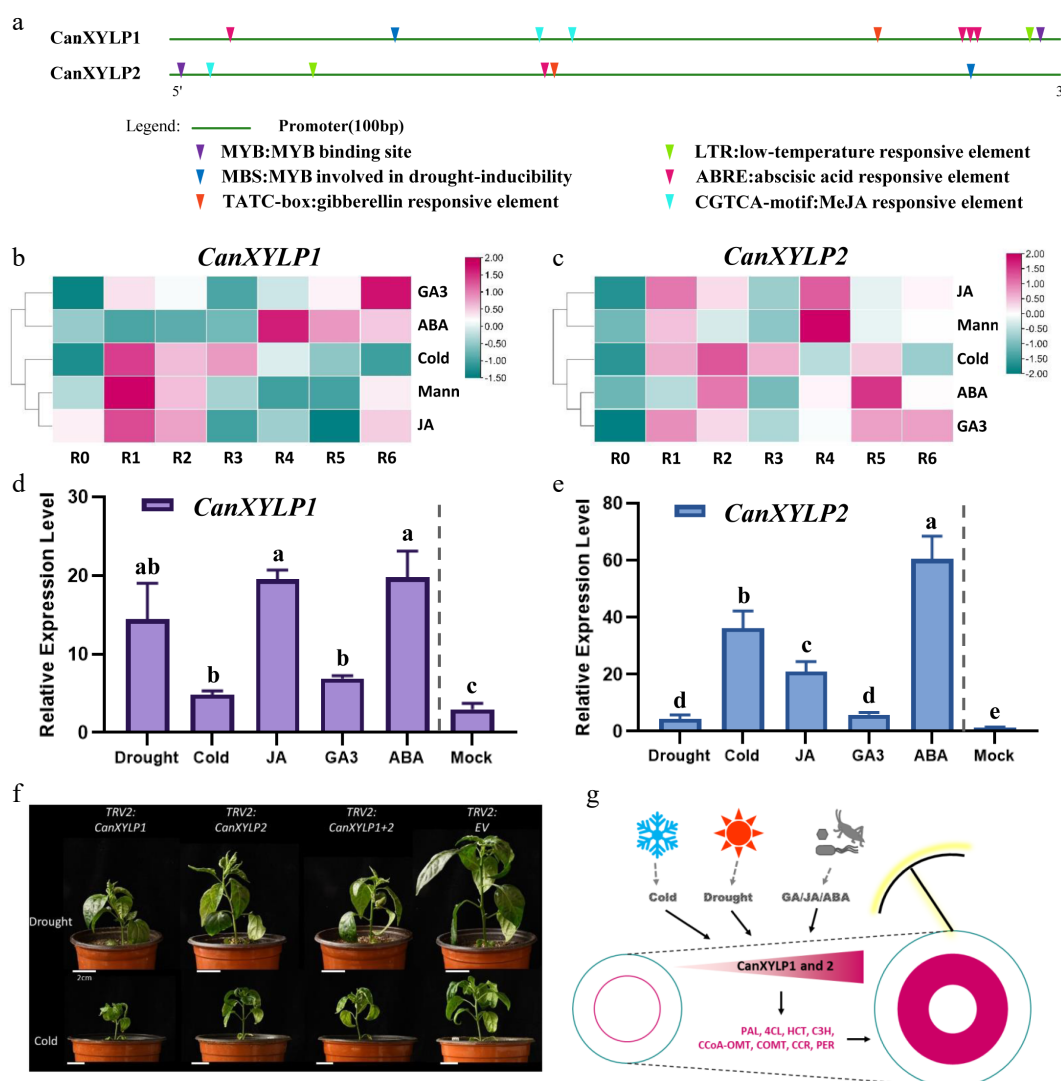


**Fig. 6** CanXYLP1 and 2 have positive responses to biotic and abiotic stresses. (a) Promoter cis-regulatory elements analysis of CanXYLP1 and CanXYLP2 promoter sequences. (b), (c) Heatmap showing the expressing level of CanXYLP1 (b) and CanXYLP2 (c) gene after biotic (GA3, ABA, JA) and abiotic (Cold, Mannitol) treatment for 1-6 hours. (d, e) qRT-PCR analysis of the relative expression levels of CanXYLP1 (d) and CanXYLP2 (e) under above biotic and abiotic treatment (equally mixed R1-R6) compared with Mock (R0) ( $P < 0.05$ ). (f) Phenotypes of TRV2:CanXYLP1/TRV2:CanXYLP2/TRV2:CanXYLP1+2/TRV2:EV + TRV1 expressed pepper plants under drought and cold stress. Bars = 2 cm. (g) Proposed model for CanXYLP1 and CanXYLP2 regulation of lignin biosynthesis during pepper stem development.



## CanXYLP1 and 2 function on stem lignification

development (Fig. 1), the expression pattern of 10 XYLP genes was also analyzed in pepper (Fig. 3). *CanXYLP1* and *CanXYLP2* expression was closely related to lignin accumulation in pepper stem growth, which inspired us to continue to explore their functions during pepper stem development. Another study showed that *xyp1xyp2* double mutant displayed the phenotype of vascular development defects in *Arabidopsis*<sup>[25]</sup>. The present study demonstrated that both *CanXYLP1* and *CanXYLP2* were crucial for pepper stem development and that either *CanXYLP1* or *CanXYLP2* gene silencing will cause lignin accumulation block in xylem (Fig. 4). The non-redundant function of XYLP1 and XYLP2 in pepper may cause their similar expression pattern, which differs from the redundant function of XYP1 and XYLP2 with different expression pattern in *Arabidopsis*<sup>[27]</sup>. Additionally, compared with *Arabidopsis*, pepper has evolved a certain number of spare genes to maintain its function normally under extreme conditions.

The present study observed that the transcript level of vital enzymes working in lignin biosynthesis pathway in the downstream of *CanXYLP1* and *CanXYLP2* had been downregulated in the *CanXYLP1/2*-silenced pepper stems (Fig. 5) and some abiotic and biotic related cis-elements in the upstream of *CanXYLP1* and *CanXYLP2*, which will influence their expression after stress treatment (Fig. 6) such as drought, low temperature, GA, JA, and ABA. The lignin content and lignification degree were regulated by a variety of biotic and abiotic responses. Under drought stress, the *ZmCAD* and *ZmCOMT* expression levels in maize (*Zea mays*) leaves increased<sup>[40]</sup>, and *ZmCCR1/2* in maize root elongation zone was significantly upregulated<sup>[41]</sup>. Additionally, drought-induced ABA and JA exhibited a positive regulatory effect on *CmCAD* gene and lignin synthesis in melon (*Cucumis melo*) stems<sup>[42]</sup>. Furthermore, low temperature affected the JA expression and lignin biosynthetic pathway-related genes in bamboo (*Phyllostachys violascens*) shoots after harvest<sup>[43]</sup>. JA, GA, and ABA are vital hormones in plants response to stresses. Shi et al.<sup>[44]</sup> exhibited that ABA could accelerate the lignification of juice sacs in pummelo (*Citrus grandis*) fruit. GA3 regulated the formation of different types of lignin in *Coleus Blumei* (*Plectranthus scutellarioides*) stems<sup>[45]</sup>. As *CanXYLP1* and *CanXYLP2* were positively regulated by stress, more lignin content will help pepper to survive stresses such as drought and chilling. MYB transcriptional factors will also play essential roles during lignin biosynthesis in horticultural plants. *CmMYB15* and *CmMYB19* enhanced lignin accumulation and resistance of chrysanthemum (*Chrysanthemum morifolium*) to aphids<sup>[46,47]</sup>. *MdMYB88* and *MdMYB124* were the causes of lignin accumulation in apple under drought stress<sup>[48]</sup>. MYB binded cis-elements in the promoter region of both *CanXYLP1* and *CanXYLP2* (Fig. 6a, purple triangle), suggesting that *CanXYLP1* and *CanXYLP2* might be regulated by MYB too.

## CONCLUSIONS

In the present study, 10 XYLP genes were identified from the pepper genome and classified into four clades according to their evolutionary relationships. Among them, the most interesting *CanXYLP1* and *CanXYLP2* have an increased expression pattern along with pepper stem development. Further experiments discovered that silencing *CanXYLP1* and *CanXYLP2* alone or together can significantly reduce lignin deposition and their upstream and downstream expression regulation, indicating

that *CanXYLP1* and *CanXYLP2* genes may be involved in lignin biosynthesis through various stresses regulation, which provide a novel insight into the characteristics of XYLPs in pepper stem lignification.

## ACKNOWLEDGMENTS

This study was supported by the National Key Research and Development Program of China (2019YFD1000301), the National Natural Science Foundation of China (32172600, 31972420) and the Fundamental Research Funds for the Central Universities (2662018QD020).

## Conflict of interest

The authors declare that they have no conflict of interest.

**Supplementary Information** accompanies this paper at (<https://www.maxapress.com/article/doi/10.48130/VR-2022-0015>)

## Dates

Received 10 August 2022; Accepted 10 October 2022; Published online 28 October 2022

## REFERENCES

1. Tripathi SC, Sayre KD, Kaul JN, Narang RS. 2003. Growth and morphology of spring wheat (*Triticum aestivum* L.) culms and their association with lodging: effects of genotypes, N levels and ethephon. *Field Crops Research* 84:271–90
2. Boerjan W, Ralph J, Baucher M. 2003. Lignin biosynthesis. *Annual Review of Plant Biology* 54:519–46
3. Vanholme R, Demedts BB, Morreel K, Ralph J, Boerjan W. 2010. Lignin biosynthesis and structure. *Plant Physiology* 153:895–905
4. Alejandro S, Lee Y, Tohge T, Sudre D, Osorio S, et al. 2012. AtABCg29 is a monolignol transporter involved in lignin biosynthesis. *Current Biology* 22:1207–12
5. Huang J, Gu M, Lai Z, Fan B, Shi K, et al. 2010. Functional analysis of the *Arabidopsis* PAL gene family in plant growth, development, and response to environmental stress. *Plant Physiology* 153:1526–38
6. Salvador VH, Lima RB, dos Santos WD, Soares AR, Böhm PA, et al. 2013. Cinnamic acid increases lignin production and inhibits soybean root growth. *PLoS ONE* 8:e69105
7. Xu B, Escamilla-Treviño LL, Sathitsuksanoh N, Shen Z, Shen H, et al. 2011. Silencing of 4-coumarate: coenzyme A ligase in switchgrass leads to reduced lignin content and improved fermentable sugar yields for biofuel production. *New Phytologist* 192:611–25
8. Ruegger M, Meyer K, Cusumano JC, Chapple C. 1999. Regulation of ferulate-5-hydroxylase expression in *Arabidopsis* in the context of sinapate ester biosynthesis. *Plant Physiology* 119:101–10
9. Vignols F, Rigau J, Torres MA, Capellades M, Puigdomènech P. 1995. The *brown midrib3* (*bm3*) mutation in maize occurs in the gene encoding caffeic acid O-methyltransferase. *The Plant Cell* 7:407–16
10. Do CT, Pollet B, Thévenin J, Sibout R, Denoue D, et al. 2007. Both caffeoyl Coenzyme A 3-O-methyltransferase 1 and caffeic acid O-methyltransferase 1 are involved in redundant functions for lignin, flavonoids and sinapoyl malate biosynthesis in *Arabidopsis*. *Planta* 226:1117–29
11. Zhang K, Qian Q, Huang Z, Wang Y, Li M, et al. 2006. *GOLD HULL AND INTERNODE2* encodes a primarily multifunctional cinnamyl-alcohol dehydrogenase in rice. *Plant Physiology* 140:972–83

12. Franke R, Hemm MR, Denault JW, Ruegger MO, Humphreys JM, et al. 2002. Changes in secondary metabolism and deposition of an unusual lignin in the *ref8* mutant of Arabidopsis. *The Plant Journal* 30:47–59
13. Vanholme B, Cesarino I, Goeminne G, Kim H, Marroni F, et al. 2013. Breeding with rare defective alleles (BRDA): a natural *Populus nigra* HCT mutant with modified lignin as a case study. *New Phytologist* 198:765–76
14. Piquemal J, Lapierre C, Myton K, O'connell A, Schuch W, et al. 1998. Down-regulation of Cinnamoyl-CoA Reductase induces significant changes of lignin profiles in transgenic tobacco plants. *The Plant Journal* 13:71–83
15. Hu D, Liu X, She H, Gao Z, Ruan R, et al. 2017. The lignin synthesis related genes and lodging resistance of *Fagopyrum esculentum*. *Biologia Plantarum* 61:138–46
16. Zhao D, Luan Y, Xia X, Shi W, Tang Y, et al. 2020. Lignin provides mechanical support to herbaceous peony (*Paeonia lactiflora* Pall.) stems. *Horticulture Research* 7:213
17. Liu Q, Luo L, Zheng L. 2018. Lignins: biosynthesis and biological functions in plants. *International Journal of Molecular Sciences* 19:335
18. Schultz CJ, Johnson KL, Currie G, Bacic A. 2000. The classical arabinogalactan protein gene family of Arabidopsis. *The Plant Cell* 12:1751–67
19. Ma Y, Yan C, Li H, Wu W, Liu Y, et al. 2017. Bioinformatics prediction and evolution analysis of arabinogalactan proteins in the plant kingdom. *Frontiers in Plant Science* 8:66
20. Mareri L, Romi M, Cai G. 2018. Arabinogalactan proteins: actors or spectators during abiotic and biotic stress in plants? *Plant Biosystems* 153:173–85
21. Sun W, Kieliszewski MJ, Showalter AM. 2004. Overexpression of tomato LeAGP-1 arabinogalactan-protein promotes lateral branching and hampers reproductive development. *The Plant Journal* 40:870–81
22. van Hengel AJ, Roberts K. 2003. AtAGP30, an arabinogalactan-protein in the cell walls of the primary root, plays a role in root regeneration and seed germination. *The Plant Journal* 36:256–70
23. Suzuki Y, Kitagawa M, Knox JP, Yamaguchi I. 2002. A role for arabinogalactan proteins in gibberellin-induced  $\alpha$ -amylase production in barley aleurone cells. *The Plant Journal* 29:733–41
24. Nguema-Ona E, Coimbra S, Vicré-Gibouin M, Mollet JC, Driouich A. 2012. Arabinogalactan proteins in root and pollen-tube cells: distribution and functional aspects. *Annals of Botany* 110:383–404
25. Motose H, Sugiyama M, Fukuda H. 2004. A proteoglycan mediates inductive interaction during plant vascular development. *Nature* 429:873–78
26. Ma T, Ma H, Zhao H, Qi H, Zhao J. 2014. Identification, characterization, and transcription analysis of xylogen-like arabinogalactan proteins in rice (*Oryza sativa* L.). *BMC Plant Biology* 14:299
27. Kobayashi Y, Motose H, Iwamoto K, Fukuda H. 2011. Expression and genome-wide analysis of the xylogen-type gene family. *Plant and Cell Physiology* 52:1095–106
28. Wang C, Chen L, Yang H, Yang S, Wang J. 2019. Genome-wide identification, expression and functional analysis of *Populus xylogen-like* genes. *Plant Science* 287:110191
29. Motose H, Sugiyama M, Fukuda H. 2001. An arabinogalactan protein(s) is a key component of a fraction that mediates local inter-cellular communication involved in tracheary element differentiation of *zinnia* mesophyll cells. *Plant and Cell Physiology* 42:129–37
30. Li T, Chen G, Zhang Q. 2021. VvXYLP02 confers gray mold resistance by amplifying jasmonate signaling pathway in *Vitis vinifera*. *Plant Signaling & Behavior* 16:1940019
31. Zhou Y, Deng Y, Liu D, Wang H, Zhang X, et al. 2021. Promoting virus-induced gene silencing of pepper genes by a heterologous viral silencing suppressor. *Plant Biotechnology Journal* 19:2398–400
32. Cuzens JC, Miller JR. 1997. Acid hydrolysis of bagasse for ethanol production. *Renewable Energy* 10:285–90
33. Ma H, Zhao J. 2010. Genome-wide identification, classification, and expression analysis of the arabinogalactan protein gene family in rice (*Oryza sativa* L.). *Journal of Experimental Botany* 61:2647–68
34. Kumar S, Stecher G, Tamura K. 2016. MEGA7: molecular evolutionary genetics analysis version 7.0 for bigger datasets. *Molecular Biology and Evolution* 33:1870–74
35. Wang Y, Tang H, Debarry JD, Tan X, Li J, et al. 2012. MCScanX: a toolkit for detection and evolutionary analysis of gene synteny and collinearity. *Nucleic Acids Research* 40:e49
36. Lescot M, Déhais P, Thijs G, Marchal K, Moreau Y, et al. 2002. PlantCARE, a database of plant *cis*-acting regulatory elements and a portal to tools for *in silico* analysis of promoter sequences. *Nucleic Acids Research* 30:325–27
37. Chen C, Chen H, Zhang Y, Thomas HR, Frank MH, et al. 2020. TBtools: an integrative toolkit developed for interactive analyses of big biological data. *Molecular Plant* 13:1194–202
38. de Oliveira Carvalho A, Gomes VM. 2007. Role of plant lipid transfer proteins in plant cell physiology—A concise review. *Peptides* 28:1144–53
39. Liu F, Yu H, Deng Y, Zheng J, Liu M, et al. 2017. PepperHub, an informatics hub for the chili pepper research community. *Molecular Plant* 10:1129–32
40. Hu Y, Li W, Xu Y, Li G, Liao Y, et al. 2009. Differential expression of candidate genes for lignin biosynthesis under drought stress in maize leaves. *Journal of Applied Genetics* 50:213–23
41. Fan L, Linker R, Gepstein S, Tanimoto E, Yamamoto R, et al. 2006. Progressive inhibition by water deficit of cell wall extensibility and growth along the elongation zone of maize roots is related to increased lignin metabolism and progressive stelar accumulation of wall phenolics. *Plant Physiology* 140:603–12
42. Liu W, Jiang Y, Jin Y, Wang C, Yang J, et al. 2021. Drought-induced ABA, H<sub>2</sub>O<sub>2</sub> and JA positively regulate *CmCAD* genes and lignin synthesis in melon stems. *BMC Plant Biology* 21:83
43. Hou D, Lu H, Zhao Z, Pei J, Yang H, et al. 2022. Integrative transcriptomic and metabolomic data provide insights into gene networks associated with lignification in postharvest Lei bamboo shoots under low temperature. *Food Chemistry* 368:130822
44. Shi M, Liu X, Zhang H, He Z, Yang H, et al. 2020. The IAA- and ABA-responsive transcription factor CgMYB58 upregulates lignin biosynthesis and triggers juice sac granulation in pummelo. *Horticulture Research* 7:139
45. Aloni R, Tollier MT, Monties B. 1990. The role of auxin and gibberellin in controlling lignin formation in primary phloem fibers and in xylem of *Coleus blumei* stems. *Plant Physiology* 94:1743–47
46. Wang Y, Sheng L, Zhang H, Du X, An C, et al. 2017. CmMYB19 overexpression improves aphid tolerance in Chrysanthemum by promoting lignin synthesis. *International Journal of Molecular Sciences* 18:619
47. An C, Sheng L, Du X, Wang Y, Zhang Y, et al. 2019. Overexpression of *CmMYB15* provides chrysanthemum resistance to aphids by regulating the biosynthesis of lignin. *Horticulture Research* 6:84
48. Geng D, Shen X, Xie Y, Yang Y, Bian R, et al. 2020. Regulation of phenylpropanoid biosynthesis by MdMYB88 and MdMYB124 contributes to pathogen and drought resistance in apple. *Horticulture Research* 7:102



Copyright: © 2022 by the author(s). Published by Maximum Academic Press, Fayetteville, GA. This article is an open access article distributed under Creative Commons Attribution License (CC BY 4.0), visit <https://creativecommons.org/licenses/by/4.0/>.